

# Magneto-optical fiber sensor based on magnetic fluid

Peng Zu,<sup>1</sup> Chi Chiu Chan,<sup>1,\*</sup> Wen Siang Lew,<sup>2</sup> Yongxing Jin,<sup>3</sup> Yifan Zhang,<sup>1</sup> Hwi Fen Liew,<sup>2</sup>  
Li Han Chen,<sup>1</sup> Wei Chang Wong,<sup>1</sup> and Xinyong Dong<sup>3</sup>

<sup>1</sup>School of Chemical & Biomedical Engineering, Nanyang Technological University, 637459 Singapore

<sup>2</sup>School of Physical & Mathematical Sciences, Nanyang Technological University, 637371 Singapore

<sup>3</sup>Institute of Optoelectronic Technology, China Jiliang University, Hangzhou, 310018 China

\*Corresponding author: ecchan@ntu.edu.sg

Received September 2, 2011; revised November 25, 2011; accepted December 4, 2011;  
posted December 6, 2011 (Doc. ID 153901); published January 30, 2012

A novel magnetic field fiber sensor based on magnetic fluid is proposed. The sensor is configured as a Sagnac interferometer structure with a magnetic fluid film and a section of polarization maintaining fiber inserted into the fiber loop to produce a sinusoidal interference spectrum for measurement. The output interference spectrum is shifted as the change of the applied magnetic field strength with a sensitivity of 16.7 pm/Oe and a resolution of 0.60 Oe. The output optical power is varied with the change of the applied magnetic field strength with a sensitivity of 0.3998 dB/Oe. © 2012 Optical Society of America

OCIS codes: 060.2370, 160.3820, 230.3810, 260.1440.

The characteristics of magneto-optical sensors are their high resolution, ultimate precision, and small size [1]. In these sensors, magneto-optical materials are the crucial components which interact directly or indirectly on the parameters of light. Magnetic fluid (MF) is an attractive magneto-optical material which possesses diverse magneto-optical effects including Faraday effect, tunable refractive index, field dependent transmission, birefringence, and so on [1]. Taking advantage of these magneto-optical properties, a lot of MF based optical devices, especially optical fiber devices, were reported [2–7]. By using the tunable refractive index property of MF, Hu proposed a current sensor with Fabry–Perot interferometer and achieved a sensitivity of 1.25 pm/Oe [2]; Dai implemented a magnetic field sensor with etched fiber Bragg grating (FBG) with a sensitivity of 0.344 pm/Oe [8]; Liu realized a tunable filter with long period grating (LPG) with a sensitivity of 4.3 pm/Oe [6]; Horng demonstrated a modulator [3]. Besides, optical switch was achieved by using the field dependent transmission property [4]. Current sensor was also carried out by using the thermal lens effect [9]. Among the various magneto-optical effects of the MF, birefringence is another important property, but few applications were reported. The challenge was that the thickness of MF film is quite small which cannot be increased significantly due to the huge absorption coefficient of MF, subsequently the phase difference caused by birefringence effect of MF is too little to be detected. Recently, many sensors based on Sagnac interferometer (SI) were reported for various parameter measurements in order to enhance the sensitivity [10–12]. Specially, the effective path length can be enhanced by combining ring resonator and SI as a birefringence magnifier, which provides a potential method to detect the small phase shift caused by MF film [13]. Previously, we reported a fiber modulator by applying MF film in the SI [7]. Efforts were made to study the modulation characteristics and improve the extinction ratio to 25 dB. However, the birefringence of MF is always accompanied by the dichroism. In this work, we focus on the sensing performance of the magnetic field sensor. It is shown by theoretical analysis the dichroism should be responsible for the decrease of the extinction ratio.

The sensitivity is improved by 1–2 orders of magnitude. The influences of MF film thickness and magnetic field direction are also discussed.

MF is a stable colloidal suspension of ferromagnetic nanoparticles in certain suitable liquid carriers. The MF used in the experiment (EMG605, Ferrotec) is a water-based ferrofluid which is fabricated by the chemical co-precipitation technique. It is a black-brown translucent liquid [1]. The nominal diameter of the nanoparticles,  $\text{Fe}_3\text{O}_4$ , was 10 nm. The volume concentration is 3.9%. The magnetic susceptibility and saturation magnetization are 2.96 Gs/Oe and 220 Oe, respectively. Under external magnetic field, the nanoparticles form chains along the magnetic field direction and the MF film exhibits optical anisotropy. When the magnetic field direction is perpendicular to the light propagating direction (perpendicular case), the effects of birefringence and dichroism in MF are dominant. When the magnetic field direction is parallel to the light propagating direction (parallel case), MF mainly shows its Faraday effect. These properties play different roles in the proposed sensor.

The sensor structure is based on a SI configuration (Fig. 1). A MF film whose plane is perpendicular to the light propagating direction, together with a 3 dB single-mode fiber (SMF) coupler and a section of 50 cm-length polarization maintaining fiber (PMF) is incorporated in the loop by means of two collimators. The magnetic field is generated by an electromagnet and calibrated by a gaussmeter. Light from an amplified spontaneous emission (ASE) source is split by the coupler. The two beams counterpropagate in the loop and interfere when they meet at the coupler again. The spectra of the sensor are measured by an optical spectrum analyzer (OSA).

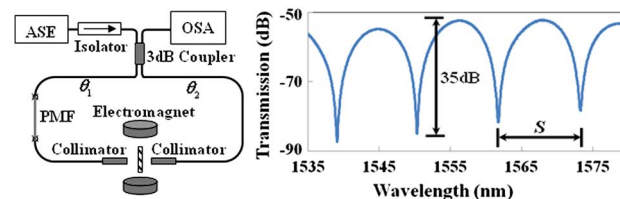


Fig. 1. (Color online) Structure of the fiber magnetic field sensor based on MF and its output spectrum.

As passing through the birefringent MF film, light is decomposed into ordinary ray (o-ray) and extraordinary ray (e-ray) and a phase difference is introduced to the e-ray and o-ray due to the birefringence effect. Meanwhile, the e-ray and o-ray are absorbed with different absorption coefficients due to the effect of dichroism. Hence, the Jones matrix of the MF film is given by

$$J = e^{-\frac{\alpha_o + \alpha_e}{2}d} \begin{pmatrix} e^{i\varphi_m/2+ad} & 0 \\ 0 & e^{-i\varphi_m/2+ad} \end{pmatrix}, \quad (1)$$

where  $\alpha_e$  and  $\alpha_o$  are the absorption coefficients for the e-ray and o-ray, respectively,  $\alpha = (\alpha_e - \alpha_o)/2$ ,  $d$  is the thickness of the MF film.  $\varphi_m = 2\pi B_m d/\lambda$  is the phase shift induced by the birefringence  $B_m$  of the MF and  $\lambda$  is the operating wavelength. With the Jones matrix method, the relative transmission spectrum  $T$  is given as [14]:

$$T = e^{-(\alpha_o + \alpha_e)d} \sin^2(\theta_1 + \theta_2) [\cosh(2ad) - \cos \varphi]/2, \quad (2)$$

where  $\varphi$  is the total phase difference caused by the MF film and PMF. If the fast axis of MF film is parallel to the fast axis of PMF,  $\varphi$  reaches its maximum  $\varphi_{\max} = \varphi_m + \varphi_P$ . If the fast axis of MF film is parallel to the slow axis of PMF,  $\varphi$  reaches its minimum  $\varphi_{\min} = \varphi_m - \varphi_P$ .  $\varphi_P$  is the phase difference caused by the PMF. Often the case, the birefringence axes of the MF and PMF are not aligned, so the value of  $\varphi$  is between  $\varphi_{\max}$  and  $\varphi_{\min}$ .  $\theta_1$  and  $\theta_2$  are the angles between the polarization direction of the input light and the birefringence axes of the MF or PMF.

Equation (2) shows  $T$  is an approximate sinusoidal function of wavelength  $\lambda$  (Fig. 1). The dip wavelength of the transmission spectrum depends on the total phase difference  $\varphi$ , which further depends on the birefringence  $B_m$  of the MF. While,  $B_m$  depends on the external magnetic field strength. Therefore, the magnetic field strength can be measured by monitoring the dip wavelength of the transmission spectrum. The period  $S$  is inversely proportional to  $\varphi$ . If  $\varphi$  is very small,  $S$  will be too large and exceed the spectrum range of light source. On the contrary, if  $\varphi$  is too large,  $S$  will be too small which means a small dynamic measurement range. In this proposed sensor, since the thickness of MF film is so small (tens of microns) that MF film itself cannot generate appropriate  $\varphi$  for measurement, a 50 cm length PMF is inserted into the Sagnac loop to provide an initial constant phase difference for offset purpose. The extinction ratio of  $T$  is dependent on the terms of  $e^{-(\alpha_o + \alpha_e)d}$  and  $\sin^2(\theta_1 + \theta_2)$ . For perpendicular case, both birefringence and dichroism properties are considered, while Faraday effect is ignored, so the dip wavelength of the spectrum will shift with the variation of the applied magnetic field strength. For parallel case, Faraday effect is considered, while birefringence and dichroism properties are ignored, but the relative small circular birefringence caused by Faraday effect will be swamped by the relative large linear birefringence of PMF, so the spectrum will not shift with the variation of the applied magnetic field strength.

The MF was sealed between two  $10 \times 10 \text{ mm}^2$  optical glasses with UV glue to form thin MF film. Three samples

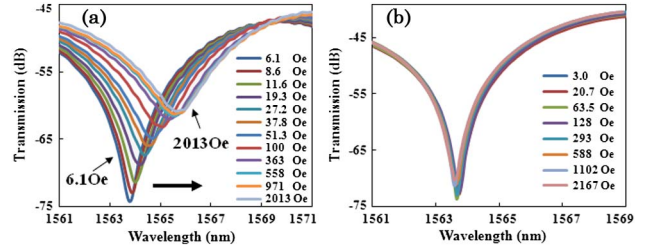


Fig. 2. (Color online) Measured spectra under different magnetic field strengths for (a) perpendicular case and (b) parallel case.

of different thicknesses (20, 30, and 60  $\mu\text{m}$ ) were prepared.

For the perpendicular case, a series of spectra were recorded in Fig. 2(a) as the magnetic field strength was increased. The initial transmission spectrum under zero magnetic field strength is indicated by “6.1 Oe” with its dip wavelength at 1563.18 nm and its extinction ratio is about 30 dB. As the magnetic field strength was increased from 0 Oe to 2013 Oe, the dip wavelength shifted to the longer wavelength side from 1563.18 nm to 1564.99 nm and the corresponding extinction ratio decreased 15 dB. The decrease of the extinction ratio was caused by the dichroism effect of the MF film.

For the parallel case, a series of spectra were recorded in Fig. 2(b) when the magnetic field strength was increased. As the magnetic field strength was increased from 0 Oe to 2167 Oe, the transmission spectrum was almost unchanged. Thus, the dip wavelength and extinction ratio of the transmission spectrum remained almost the same for different magnetic field strengths.

In order to analyze the influence of different MF film thicknesses on the performance of the sensor, the experiments were repeated for the other two samples (20 and 60  $\mu\text{m}$ ). The relationships between the dip wavelengths and the magnetic field strengths were recorded in Fig. 3. For perpendicular case, when the magnetic field strength was smaller than 300 Oe, the dip wavelength shifted quickly and linearly as the magnetic field strength increasing. When the magnetic field strength was larger than 400 Oe, the dip wavelength shift was gradually saturated. The data can be fit well by the modified Langevin function. For the case of small magnetic field strength, linear fit was applied. For the MF films of 20, 30, and 60  $\mu\text{m}$ , the corresponding sensitivities are 6.4, 11.4,

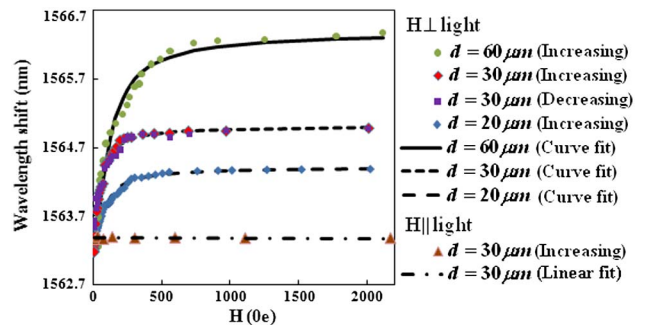


Fig. 3. (Color online) Dip wavelength of the spectrum varies with the external magnetic field strength for perpendicular case and parallel case.

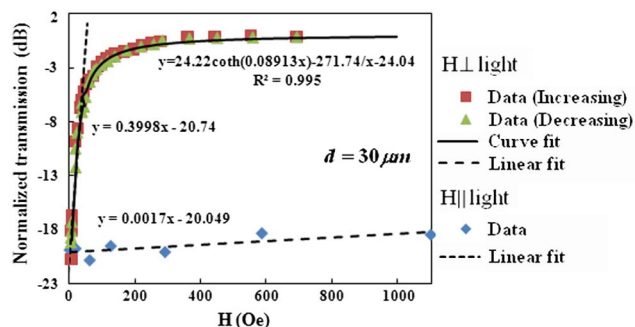


Fig. 4. (Color online) Normalized transmission power varies with external magnetic field strength for perpendicular case and parallel case.

and 16.7 pm/Oe, respectively and the corresponding resolutions are 1.56, 0.88, and 0.60 Oe, respectively, at the resolution limit of 10 pm of the OSA. For the MF film of 60  $\mu\text{m}$ , its sensitivity is about one order of magnitude better than the result of the current sensor based on Fabry–Perot interferometer (FPI) [2] and the result of the filter based on LPG [6], two orders of magnitude better than the result of the magnetic field sensor based on etched FBG [8]. Figure 3 shows the linear range of the proposed sensor for different thicknesses of MF films are the same, about 300 Oe, which depends on the properties of the MF such as concentration. The dynamic range is independent on the thickness of MF film, but can be enhanced by increasing the concentration of the MF. Rapidly increasing and decreasing the magnetic field strength, the data in Fig. 3 almost coincide, which means the sensor has a good repeatability. For the parallel case, the dip wavelength was almost unchanged. Compared to the perpendicular case, the sensitivity is estimated to be  $-9 \times 10^{-4}$  pm/Oe, which can be neglected.

A tunable laser source (TLS) and powermeter were used to test the sensor for benefiting dynamic sensing applications. In order to obtain the best sensitivity, the output wavelength of TLS was tuned to one of the dip wavelengths under zero magnetic field strength (e.g., 1563.18 nm in Fig. 2(a)). Hence, as the applied magnetic field strength changes, the corresponding output power will change accordingly. The normalized transmission power is shown in Fig. 4. For perpendicular case, the data can be fit well by modified Langevin function with a high  $R^2$  value of 0.995. The sensitivity was estimated to be 0.3998 dB/Oe. The repeatability was verified, too. For parallel case, the output power was not as stable as the measurement of the dip wavelength. The sensitivity was 0.0017 dB/Oe, which was 235 times smaller than the one of the perpendicular case. The time response property of

the sensor is mainly determined by the response time of the MF, which was reported in the range of 10–30 ms [3]. Therefore, the highest frequency of the dynamic magnetic field the sensor can measure is about 100 Hz.

In conclusion, the magnetic field sensor based on the birefringence property of the MF film is demonstrated. The performance of the sensor is related to the magnetic field direction, so the sensor is performed in the perpendicular case and the parallel case, respectively. For the perpendicular case, the dip wavelength of the output spectrum shifts with the change of the applied magnetic field strength. The results show the thicker the MF film, the higher the sensitivity and the resolution. The best sensitivity and resolution achieved for the 60  $\mu\text{m}$  thickness MF film are 16.7 pm/Oe and 0.60 Oe, respectively. The sensor can also be operated as dynamic magnetic field sensor in the frequency response range about 100 Hz with a sensitivity of 0.3998 dB/Oe with good repeatability. On the other hand, both the dip wavelength and the output intensity almost remain unchanged with the variation of the applied magnetic field strength for the parallel case. The proposed structure of the magnetic field sensor also has some potential applications such as modulators and switches.

## References

1. L. Martinez, F. Cecelja, and R. Rakowski, *Sens. Actuators A* **123–24**, 438 (2005).
2. T. Hu, Y. Zhao, X. Li, J. Chen, and Z. Lv, *Chinese Opt. Lett.* **8**, 392 (2010).
3. H. E. Horng, J. J. Chieh, Y. H. Chao, S. Y. Yang, C. Y. Hong, and H. C. Yang, *Opt. Lett.* **30**, 543 (2005).
4. H. E. Horng, C. S. Chen, K. L. Fang, S. Y. Yang, J. J. Chieh, C. Y. Hong, and H. C. Yang, *Appl. Phys. Lett.* **85**, 5592 (2004).
5. J. J. Chieh, S. Y. Yang, H. E. Horng, C. Y. Hong, and H. C. Yang, *Appl. Phys. Lett.* **90**, 133505 (2007).
6. T. Liu, X. Chen, Z. Di, J. Zhang, X. Li, and J. Chen, *Appl. Phys. Lett.* **91**, 121116 (2007).
7. P. Zu, C. C. Chan, L. W. Siang, Y. X. Jin, Y. F. Zhang, L. H. Fen, L. H. Chen, and X. Y. Dong, *Opt. Lett.* **36**, 1425 (2011).
8. J. X. Dai, M. H. Yang, X. B. Li, H. L. Liu, and X. L. Tong, *Opt. Fiber Technol.* **17**, 210 (2011).
9. S. H. Yuan and X. W. Chen, in *Fiber Optic Sensors V*, K. D. Bennett, B. Y. Kim, and Y. B. Liao, eds. (Spie—Int Soc Optical Engineering, 1996), pp. 8–10.
10. P. Zu, C. C. Chan, Y. X. Jin, Y. F. Zhang, and X. Y. Dong, *Meas. Sci. Technol.* **22**, 025204 (2011).
11. P. Zu, C. C. Chan, Y. X. Jin, T. X. Gong, Y. F. Zhang, L. H. Chen, and X. Y. Dong, *IEE. Photon. Technol. Lett.* **23**, 920 (2011).
12. O. Frazo, J. Baptista, and J. Santos, *Sensors* **7**, 2970 (2007).
13. I. Golub and E. Simova, *Opt. Lett.* **30**, 87 (2005).
14. I. Golub and E. Simova, *Opt. Lett.* **27**, 1681 (2002).